

An Overview of Parametric Modeling and Methods for Radar Target Detection with Limited Data

Wang, Fangzhou; Wang, Pu; Zhang, Xin; Li, Hongbin; Himed, Braham

TR2021-049 May 12, 2021

Abstract

This article provides a survey of recent results on exploiting parametric auto-regressive (AR) models for adaptive radar target detection. Specifically, three types of radar systems are considered, including phased-array radar with multiple co-located transmitters and receivers, distributed multi-input multi-output (MIMO) radar with widely and spatially separated transmitters and receivers, and passive radar which uses existing sources as illuminators of opportunity (IOs). These radar systems are of significant interest for a wide range of military and civilian applications. For each of the three types of radars, we discuss how AR processes can be employed to succinctly model the underlying signal correlation and efficiently estimate it from limited data, thus enabling effective target detection in complex non-homogeneous environments when training data is limited. We illustrate the performance of such parametric model assisted detectors relative to conventional non-parametric approaches by using computer simulated and experimental data.

IEEE Access

An Overview of Parametric Modeling and Methods for Radar Target Detection with Limited Data

Fangzhou Wang, Pu Wang, *Senior Member, IEEE*, Xin Zhang, *Member, IEEE*, Hongbin Li, *Fellow, IEEE*, and Braham Himed, *Fellow, IEEE*

Abstract—This article provides a survey of recent results on exploiting parametric auto-regressive (AR) models for adaptive radar target detection. Specifically, three types of radar systems are considered, including phased-array radar with multiple co-located transmitters and receivers, distributed multi-input multi-output (MIMO) radar with widely and spatially separated transmitters and receivers, and passive radar which uses existing sources as illuminators of opportunity (IOs). These radar systems are of significant interest for a wide range of military and civilian applications. For each of the three types of radars, we discuss how AR processes can be employed to succinctly model the underlying signal correlation and efficiently estimate it from limited data, thus enabling effective target detection in complex non-homogeneous environments when training data is limited. We illustrate the performance of such parametric model assisted detectors relative to conventional non-parametric approaches by using computer simulated and experimental data.

Index Terms—Parametric modeling, adaptive target detection, phased-array radar, distributed multi-input multi-output (MIMO) radar, passive radar

I. INTRODUCTION

Parametric modeling is frequently used in the design and analysis of radar systems (e.g., [1]–[10]). It employs physical or statistical models consisting of a finite number of parameters that are useful in the representation and processing of a signal for radar functions. There are many parametric models available for radar applications, e.g., geometrical theory of diffraction model [1], hidden Markov model [2], compound Gaussian model [3], and auto-regressive (AR) model [4]–[10], etc. The AR model has attracted extensive research efforts for radar target detection since it can fit both Gaussian and non-Gaussian observations. In addition, parameter estimation of the AR model is relatively simple, which usually involves solving a system of linear equations.

Adaptive target detection is a fundamental topic for radar engineers. The problem involves detecting a weak target signal from strong interference. Effective interference cancellation requires some accurate knowledge, e.g., the covariance matrix of the interference. Many adaptive detection algorithms, such

as the well-known sample matrix inversion (SMI) detector [11] and Kelly’s generalized likelihood ratio test (GLRT) [12], need a large amount of homogeneous training (secondary) data to obtain an accurate estimate of the clutter covariance matrix. However, real-world radar interference is often non-homogeneous, which precludes the availability of adequate training data for covariance matrix estimation. We consider radar detection in such scenarios with *limited data*, i.e., lack of sufficient training data for interference estimation. The problem can be addressed by utilizing a suitable parametric model for the interference. This article reviews some recent developments on exploiting parametric AR models for target detection in three different types of radar systems with limited data, namely phased-array radar, distributed multi-input multi-output (MIMO) radar, and passive radar, respectively.

A standard phased-array radar can be considered as a single-input multi-output (SIMO) system, where a single waveform is radiated and the returned signal is collected via multiple receiving antenna elements. Space-time adaptive processing (STAP) techniques, which have been developed for adaptive target detection in phased-array radar and are mostly used assuming homogeneity of the training data, have shown significant performance loss in non-stationary/non-homogeneous interference environments of unknown statistics [14]. One way to solve the inhomogeneity related problem is to use data selection techniques based on either knowledge-based criteria or data-adaptive methodologies [15]–[17]. Another different strategy to reduce training requirements in STAP is to utilize a suitable AR model for the clutter and exploit the parametric model for target detection. In particular, multi-channel AR models have been found to be very effective in representing the temporal correlation among different types of clutter signals [18]. Thus, several parametric detectors were developed by modeling the clutter as an AR process which exploits the structural information of the clutter covariance [5]–[10], [19]–[21]. AR model based estimation of clutter parameters is closely related to multi-stage Wiener filtering through conjugate-gradient (CG) iterations, which has led to the development of several CG-based parametric detectors [22], [23].

Distributed MIMO radar that employs multiple widely separated antennas within the transmit and receive aperture, illuminates a target from different spatial aspects, which provides the ability to enhance performance by exploiting the spatial or geometric diversity [24]–[27]. However, the non-homogeneous problem in such a system is even worse than the phased-array radar due to the multistatic configuration. Specifically, the non-

This work was supported in part by the National Science Foundation under grants ECCS-1609393 and ECCS-1923739. The work of P. Wang was done when he was with Stevens Institute of Technology.

Fangzhou Wang, Xin Zhang, and Hongbin Li are with the Department of Electrical and Computer Engineering, Stevens Institute of Technology, Hoboken, NJ 07030 USA (fwang11@stevens.edu; zhangx1252@gmail.com; hli@stevens.edu).

Pu Wang is with Mitsubishi Electric Research Laboratories (MERL), 201 Broadway, Cambridge, MA 02139, USA (e-mail: pwang@merl.com).

Braham Himed is with AFRL/RYMD, Dayton, OH 45433 USA (email: braham.himed@us.af.mil).

homogeneity of the clutter is caused by two factors, including the azimuth-selective backscattering of the clutter scatterers observed by different transmit-receive (Tx-Rx) antenna pairs as well as the non-stationary clutter covariance structure across resolution cells [28]. This issue can be addressed by using a set of independent scalar AR processes to model the clutter observed by different Tx-Rx pairs, which accounts for the inhomogeneity of the first type [29], [30]. With the parametric modeling of the disturbance, there is no need to use range training data from adjacent resolution cells to estimate the clutter covariance matrix, which bypasses the inhomogeneity across resolution cells in a neighborhood.

Passive radar seeks to exploit a readily available illuminator of opportunity (IO), e.g., frequency modulation (FM) radio, television, and digital audio/video broadcasting, to detect and track targets of interest [31]–[33]. Passive radar is more covert and provides reduced RF pollution to the electromagnetic environment since it does not need a transmitter. However, this also imposes an additional challenge due to the non-cooperative nature of the system, since the transmitted signal is generally unknown at the receiver [34]. The unknown IO waveform can be treated as either a deterministic signal or a stochastic signal [35], [36]. Due to coding, modulation, pulse shaping, and propagation effects, the IO waveform is generally correlated and such temporal correlation can be exploited by modeling the waveform as an AR process to improve the detection performance [37]–[39].

In the remainder of this paper, we detail how AR models can be leveraged for parametric detection in phased-array radar (Section II), distributed MIMO radar (Section III), and passive radar (Section IV). We offer some concluding remarks in Section V.

Notations: We use boldface symbols for vectors (lower case) and matrices (upper case). $(\cdot)^T$ denotes the transpose and $(\cdot)^H$ the conjugate transpose. $\mathcal{CN}(\mathbf{u}, \Sigma)$ denotes the complex Gaussian distribution with mean \mathbf{u} and covariance matrix Σ . $\mathbb{C}^{N \times 1}$ denotes the set of $N \times 1$ complex vectors. $\lfloor x \rfloor$ is the floor function that outputs the greatest integer less than or equal to x .

II. PARAMETRIC DETECTION FOR PHASED-ARRAY RADAR

Consider a phased-array radar that employs J antennas to transmit a coherent burst of pulses at a constant pulse repetition frequency (PRF) $f_r = 1/T_r$, where T_r is the pulse repetition interval (PRI). The transmitter carrier frequency is $f_c = c/\lambda$, where c is the speed of light and λ is the wavelength. The time interval over which the waveform returns are collected is commonly referred as the coherent processing interval (CPI). The CPI length is equal to KT_r where K is the number of pulses in the CPI. At the radar receiver, each antenna has its own down-converter, matched filter, and analog-to-digital converter (ADC). Matched filtering is performed separately on the returns from each pulse, after which the signals are sampled by the ADC to create *slow-time* and *fast-time* samples [40]. Slow-time samples are taken at the PRF, while fast-time samples are taken at a sampling rate determined by the bandwidth of the radar waveform and

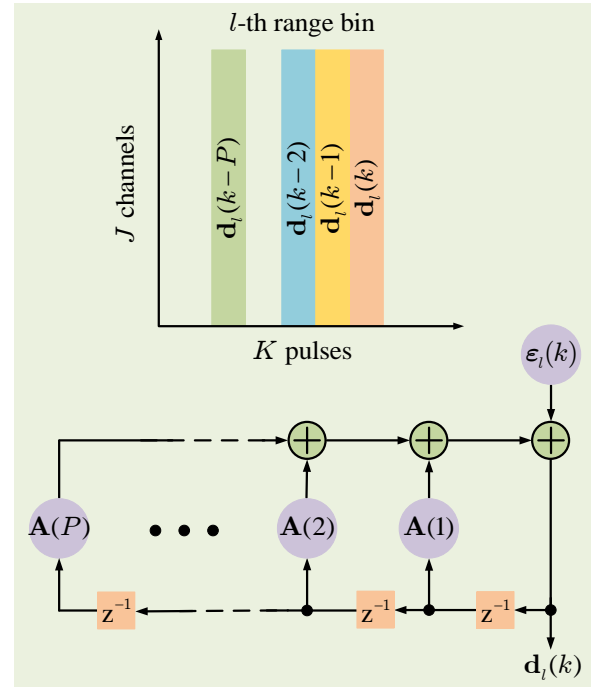


Figure 1. J -channel AR(P) process: The $J \times 1$ vector $\mathbf{d}_\ell(k)$ is the spatial snapshot of the disturbance at the ℓ -th range bin and k -th pulse. It is modeled as an AR process with coefficients $\{\mathbf{A}(p)\}_{p=1}^P$ and spatial noise vector $\boldsymbol{\varepsilon}_\ell(k)$.

each fast-time sample corresponds to a specific range bin. The slow/fast-time sampling along with spatial sampling performed by the antenna elements result in a *data cube*. A fundamental problem for the radar is to detect whether targets are present in each range bin. Let $\mathbf{x}_0(k) \in \mathbb{C}^{J \times 1}$ contain the J spatial samples collected at the k -th pulse for a test range bin. The target detection problem is to select between two hypotheses in the presence of spatially and temporally correlated disturbance [8]:

$$\begin{aligned} H_0 : \quad & \mathbf{x}_0(k) = \mathbf{d}_0(k), \\ H_1 : \quad & \mathbf{x}_0(k) = \alpha \mathbf{s}(k) + \mathbf{d}_0(k), \quad k = 0, 1, \dots, K-1, \end{aligned} \quad (1)$$

where $\mathbf{s}(k)$ is the known target steering vector which is the response of the system to a unit amplitude target, α is the unknown target amplitude, and $\{\mathbf{d}_0(k)\}_{k=0}^{K-1}$ are the disturbance signals (i.e., clutter and noise) that are in general correlated in space and time. Particularly, $\mathbf{s}(k)$ depends on the array geometry and is parameterized by the target spatial frequency w_s and the normalized Doppler frequency w_d . For a uniformly spaced linear array (ULA), the j -th element of the target steering vector $\mathbf{s}(k)$ is given by $e^{j2\pi(j-1)w_s} e^{j2\pi(k-1)w_d}$. For training-based detectors, it is assumed that there is a set of target-free training signals $\mathbf{x}_\ell(n)$, $\ell = 1, \dots, L$, which are often signals from range bins that are close to the test range bin.

The detection problem in (1) can be solved by employing either a covariance matrix based approach [11], [12] or a parametric method [5]–[9]. Here, the structural information of the disturbance covariance matrix is exploited to improve the detection performance and reduce the training requirement. More precisely, as shown in Fig. 1, the disturbance signal

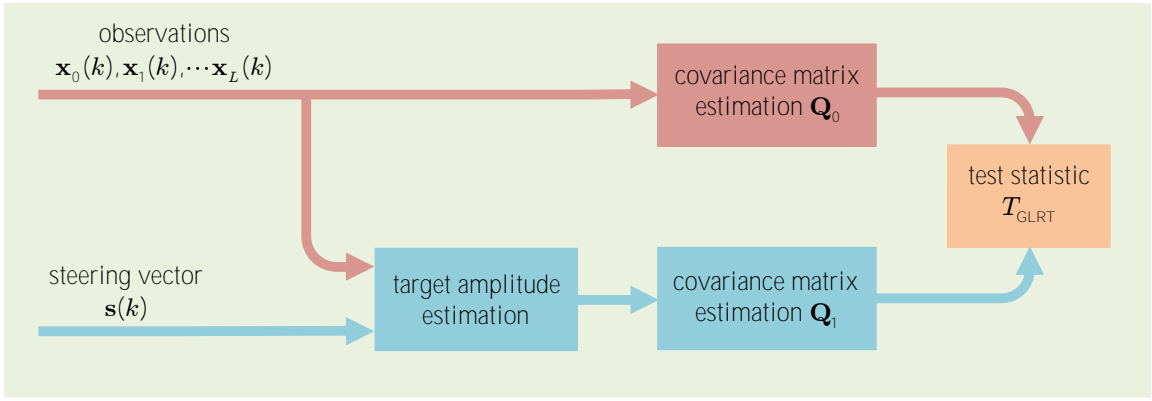


Figure 2. Parametric detector for STAP phased-array radar.

$\{\mathbf{d}_\ell(k)\}_{\ell=0}^J$ is modeled as a J -channel AR process with known model order P :

$$\mathbf{d}_\ell(k) = - \sum_{p=1}^P \mathbf{A}^H(p) \mathbf{d}_\ell(k-p) + \varepsilon_\ell(k), \quad (2)$$

where $\{\mathbf{A}(p)\}_{p=1}^P$ denote the unknown $J \times J$ AR coefficient matrices to be estimated and $\varepsilon_\ell(k)$ denotes the $J \times 1$ spatial noise vectors that are temporally white but spatially colored Gaussian noise: $\varepsilon_\ell(k) \sim \mathcal{CN}(\mathbf{0}, \mathbf{Q})$, where \mathbf{Q} is the unknown $J \times J$ spatial covariance matrix.

The multi-channel AR model in (2) has been used to develop parametric STAP detectors in several efforts [5]–[8]. In the following, we discuss a parametric GLRT [13]. First, the GLRT is evaluated by expressing the likelihood ratio as a function of unknown parameters: the target amplitude α , AR coefficient matrices $\{\mathbf{A}(p)\}_{p=1}^P$, and the spatial covariance matrix \mathbf{Q} . Subsequently, the likelihood function under each hypothesis is maximized to yield the maximum likelihood estimates (MLEs) of the unknown parameters, which are then used to replace the unknown parameters in the likelihood ratio and compute the test statistics. The flowchart of the parametric GLRT is shown in Fig. (2). The amplitude estimation under H_1 turns out to be the key problem since the other parameters can be readily obtained once an estimate of α is available. However, the cost function of the maximum likelihood (ML) amplitude estimator is highly non-linear. Newton-like iterative searches are usually used to find the MLE of the amplitude. A sub-optimum but computationally more efficient estimator, referred to as the asymptotic ML (AML) estimator, can be used to construct a simplified parametric GLRT. It can be shown that, with the parametric AR modeling of the disturbance, the parametric GLRT reduces to a ratio of the determinants of the ML estimates of spatial covariance matrices under the two hypotheses [8]:

$$T_{\text{GLRT}} = \frac{|\hat{\mathbf{Q}}_0|_{H_1}}{|\hat{\mathbf{Q}}_1|_{H_0}} \underset{H_0}{\overset{H_1}{\gtrless}} \gamma_{\text{GLRT}}, \quad (3)$$

where γ_{GLRT} denotes the test threshold to meet a preset probability of false alarm, and $\hat{\mathbf{Q}}_0$ and $\hat{\mathbf{Q}}_1$ are the MLEs of the spatial covariance matrix \mathbf{Q} under the null and alternative hypotheses, respectively.

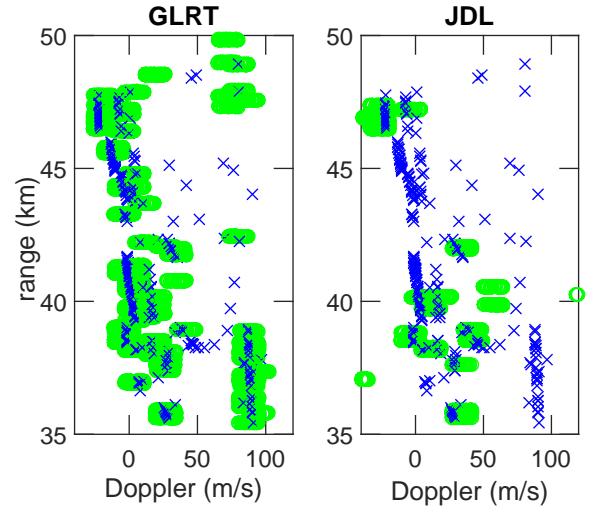


Figure 3. Detection maps of (a) the parametric GLRT, and (b) the JDL detector for the KASSPER dataset. The true targets are represented by blue cross signs and the detections (range-Doppler cells with test statistics exceeding the detection threshold) are shown in green bars.

To illustrate the merit of parametric modeling in the STAP detection problem, we present test results using data from KASSPER [41] and MCARM [42]. This allows us to assess the influence from the mismatch between the AR model assumption and the real disturbance.

1) *KASSPER Dataset*: The KASSPER 2002 dataset contains many real-world effects including heterogeneous terrain, array errors, and dense ground targets. The simulated airborne radar was flying at 3000 meters altitude and speed of 100 m/s, traveling east with a 3° crab angle. The radar was operating at 1240 MHz with a peak power of 15 kW. The 11 virtual antenna array elements were spaced slightly less than a half-wavelength apart at 0.1092 m (0.9028 half-wavelength spacing), and the transmit array is uniformly weighted in the horizontal dimension and phased to steer the mainbeam to 195°. The PRF was 1984 Hz and the CPI contains 32 pulses. The KASSPER dataset simulates a dense target environment. Of particular interest are the targets in the mainbeam of the radar within the range swath of interest. In total, there are 268 targets in the range interval between 35 km and 50 km.

We apply the parametric GLRT detector to the KASSPER

data of interest and compute the test statistics with respect to Doppler frequency and range cells. To compare with other techniques, we count the number of detection while setting the threshold with a constraint on the number of false alarm. Due to range/Doppler sidelobes resulting from pulse compression and Doppler filtering, it is common for a target to spread into nearby range-Doppler bins. For this reason, it is a standard procedure for a radar to cluster target detections such that a detection in a given range-Doppler cell is associated with a target that lies in a contiguous range cell or Doppler bin. For the results reported here, we cluster ± 1 cells in range and ± 1 bands in Doppler for all processing schemes. Once we declare a detection in its region, the corresponding test value is removed from the original test statistics to avoid over-counting. For comparison purposes, the Joint Domain Localized (JDL) technique [43], [44] with 3×3 local processing region (LPR) is applied to the KASSPER dataset. There are 64 Doppler frequency bands and two guard cells are used at each side of the test range cell. The number of false alarm N_{fa} is constrained to 10. To improve the detection performance, we limit the training data by applying the Innovation Power Sorting (IPS) technique [45]. When $J = 11$, $L = 22$, and $P = 2$, the detection maps for the parametric GLRT and JDL are shown in Fig. 3. The results show that the parametric GLRT can detect 102 targets while JDL can detect 25 targets.

2) *MCARM Dataset*: In this section, the MCARM dataset obtained from a real-world multi-channel airborne experiment, and contains clutter in various terrains including mountains, rural, urban, and land/sea interface, is considered. The MCARM data was collected from a BAC 1-11 airborne platform operating at L-Band. The MCARM array has 16 columns and each column consists of two four-element sub-arrays. Each sub-array has its own output or is combined into a single output per column with up to 24 outputs for the array. Since the true joint space-time covariance matrix of the MCARM dataset is unavailable, a power measure, called *input SINR* (per-pulse, per-channel), is adopted and will be computed from the data. It is defined as $\text{SINR} = |\alpha|^2/\sigma_d^2$, where α is the target amplitude and σ_d^2 denotes the variance (power) of each element of the disturbance vector at each time instant. The MCARM database, specifically acquisition rd050575, has been used extensively to assess the performance of the parametric GLRT approach. To test the detection performance potential, an artificial target with an SINR of -30 dB is injected in the range bin 295. The disturbance power σ_d^2 is estimated as a five-bin average centered on the range bin in which the target is placed. Model order values $P = 1, 2, 3, 4$ were evaluated for each parametric test and the model with the best performance was selected. The selection criterion is the difference between the target peak value and the highest non-target peak value. Diagonal loading of 40 dB for the adaptive matched filter (AMF) detector [46] is applied. Fig. 4 shows the test statistics for the three considered detectors. It is seen that the parametric GLRT can detect the target with a gain of 23 dB even without training ($L = 0$), while JDL has a gain of 18.5 dB with $L = 8$ training signals, but the AMF fails to declare a detection with $L = 8$.

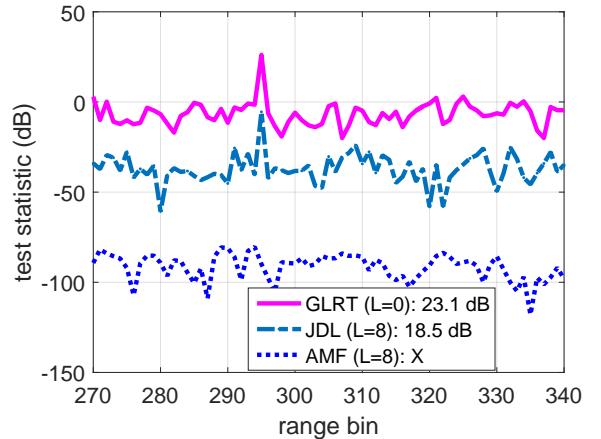


Figure 4. The test statistics of detectors for the MCARM dataset with $J = 4$ spatial channels, $K = 128$ pulses, and no ($L = 0$) or limited ($L = 8$) limited training data.

III. PARAMETRIC DETECTION FOR DISTRIBUTED MIMO RADAR

Observing targets over wide angular sectors with distributed MIMO radar offers great benefits for Doppler processing and moving target detection (MTD) [24]. Compared with traditional monostatic or bistatic radar, distributed MIMO radar is particularly useful when the targets are difficult to distinguish from the background clutter by a single illumination path, i.e., targets with low radial velocities or blind speeds [47]. Moreover, the joint processing of the received signals in MIMO radar provides further performance improvement compared to multistatic radar, referring here to the case where each receiver performs its own Doppler estimation.

Consider the detection of a moving target using a distributed MIMO radar [24]–[26], [29]. Without loss of generality, assume a moving target with a velocity $\mathbf{v} \triangleq (v_x, v_y)$ is in the same 2-dimensional (2-D) plane of the transmit and receive antenna elements of the distributed MIMO radar system. The techniques discussed in the sequel can be easily extended to the 3-D case [29]. The transmit and receive antennas are assumed to be on stationary platforms. The relative geometry of the setup is illustrated in Fig. 5. Let the target be illuminated by M transmit antennas with illumination angles θ_{vm} , $m = 1, \dots, M$. The signals scattered by the target are collected by N receive antennas placed at locations of direction θ_{rn} , $n = 1, \dots, N$. Given the M transmitters and N receivers, there are MN Tx-Rx paths, resulting in MN different spatial looks of the resolution cell under test. To exploit target spatial diversity for detection, the M transmit waveforms are assumed to be orthogonal for ease of separation at the receiver. The same approach as that used in standard Doppler radars which employs pulsed transmission is used here [40]. Each transmitter in the MIMO radar system sends a succession of K periodic pulses, i.e., K repetitions of an orthogonal waveform over a CPI. Each receiver employs a bank of M matched filters corresponding to M orthogonal waveforms. The matched filter output is sampled at the pulse repetition interval (PRI) via slow-time sampling. A vector $\mathbf{x}_{mn} \in \mathbb{C}^{K \times 1}$ contains K samples of the matched filter output

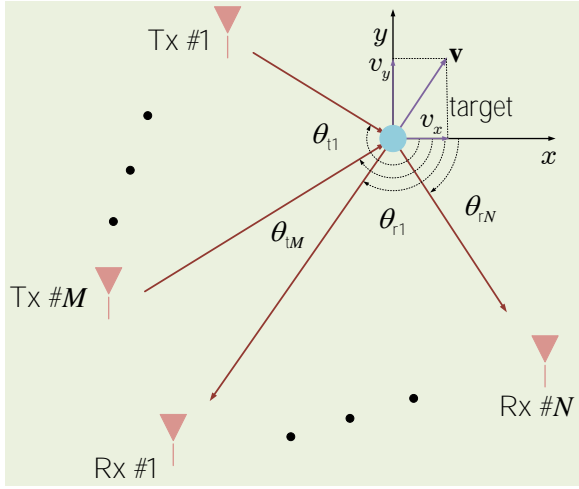


Figure 5. Distributed MIMO radar configuration for moving target detection.

(within a CPI) at the n -th receiver matched to the transmitted waveform from the m -th transmitter. The detection problem is then to test the presence of the moving target in the cell of interest using the observations $\{\mathbf{x}_{mn}\}$.

Specifically, the target detection problem involves selecting between the following two hypotheses [29]:

$$\begin{aligned} H_0: \quad & \mathbf{x}_{mn} = \mathbf{d}_{mn}, \\ H_1: \quad & \mathbf{x}_{mn} = \alpha_{mn} \mathbf{s}(f_{mn}) + \mathbf{d}_{mn}, \end{aligned} \quad (4)$$

$$n = 1, \dots, N; m = 1, \dots, M,$$

where α_{mn} denotes the unknown signal amplitude associated with the (m, n) -th Tx-Rx pair and \mathbf{d}_{mn} is the clutter and noise components. With widely separated antennas, the amplitude α_{mn} varies significantly with aspect angle, due to the azimuth-selective backscattering [24]. Thus, $\{\alpha_{mn}\}$, which are different for different Tx-Rx pairs, are modeled as deterministic unknown parameters. In addition, \mathbf{d}_{mn} is the disturbance signal that integrates the clutter and noise. Further, $\mathbf{s}(f_{mn})$ is a $K \times 1$ steering vector with the k -th element given by $e^{-j2\pi(k-1)f_{mn}}$, where f_{mn} denotes the normalized Doppler frequency such that (cf. Fig. 5)

$$f_{mn} = \frac{T_r}{\lambda} [v_x (\cos \theta_{tm} + \cos \theta_{rn}) + v_y (\sin \theta_{tm} + \sin \theta_{rn})], \quad (5)$$

where T_r denotes the PRI. The moving target is assumed to be in the far field such that the Doppler shift with respect to the antennas is constant within the CPI.

Due to the multistatic configuration inherent in distributed MIMO radar, it is straightforward to consider the disturbance signals from different Tx-Rx pairs as non-homogeneous [48], [49]. In order to account for the non-homogeneous disturbance, a set of MN different AR processes can be employed to model the disturbance signal seen by different Tx-Rx pairs. These independent AR processes are capable of modeling variations in both the clutter structure and power level across different probing-observing angles in distributed MIMO radar [29]. Specifically, the k -th slow-time sample of the disturbance for the (m, n) -th Tx-Rx pair, i. e., $d_{mn}(k)$, is modeled as a

scalar AR process with model order P_{mn} :

$$d_{mn}(k) = - \sum_{p=1}^{P_{mn}} a_{mn}(p) d_{mn}(k-p) + \varepsilon_{mn}(k), \quad (6)$$

where $a_{mn}(p)$ denotes the p -th AR coefficient and $\varepsilon_{mn}(k) \sim \mathcal{CN}(0, \sigma_{mn}^2)$ is the zero-mean driving noise with variance σ_{mn}^2 .

To test for the presence of a target in a resolution cell, a parametric detection solution can be developed by using the above AR model, e.g., a parametric detector that maximizes the likelihood function under both hypotheses in (4) over the unknown parameters including target amplitudes α_{mn} , velocities v_x and v_y , driving noise variance σ_{mn}^2 , and the AR coefficients $\{a_{mn}(p)\}_{p=1}^{P_{mn}}$. Note that the MLE of the target velocity requires a 2-D optimization that can be solved through numerical approaches [25]. The other parameters can then be obtained via least squares. Finally, the parametric GLRT detector for MIMO radar, referred as MIMO-PGLRT, can be obtained by substituting all the parameter estimates back into the likelihood ratio. It can be shown that the detector performs local adaptive subspace detection, non-coherent combining using local decision variables, and a global threshold comparison, as shown in Fig. 6 [29]. Specifically, a test statistic is computed at each sensor by first adaptively projecting the test signal \mathbf{x}_{mn} into two distinct subspaces and then computing the energy of both projected test signals. The aggregate statistic which is obtained through a non-coherent combination of the test statistic computed at each sensor is compared with the global threshold. The two distinct subspaces are the orthogonal complement of a regression data matrix formed using the return signal within a CPI under hypothesis H_1 and the alternative hypothesis, respectively.

The MIMO-PGLRT detector does not require any training data. For comparison, we also consider two conventional covariance matrix based detectors, both depending on training. The first detector is the sample covariance matrix (SCM)-based detector [24]. This method requires L homogeneous training signals for each transmit-receive pair to form a pairwise disturbance covariance matrix

$$\hat{\mathbf{C}}_{mn} = \frac{1}{L} \sum_{\ell=1}^L \mathbf{x}_{mn,\ell} \mathbf{x}_{mn,\ell}^H, \quad (7)$$

where $\mathbf{x}_{mn,\ell} \in \mathbb{C}^{K \times 1}$ denotes the ℓ -th training signal for the (m, n) -th Tx-Rx pair. The covariance matrix $\hat{\mathbf{C}}_{mn}$ is used to whiten the observation \mathbf{x}_{mn} prior to cross correlating it with the Doppler steering vector $\mathbf{s}(f_{mn})$. To ensure that the sample covariance matrix is full rank, $L > K$ range training signals are required for each transmit-receive pair. In general, $L = 2K$ training signals are needed for an acceptable performance. As such, the SCM detector requires at least $2KMN$ training signals in total, which may be difficult to fulfill in a non-homogeneous environment.

The second detector is the robust MIMO detector [26], which employs a compound-Gaussian model for both the test and training signals across different Tx-Rx pairs to address non-homogeneous training. The detector uses a fixed-point

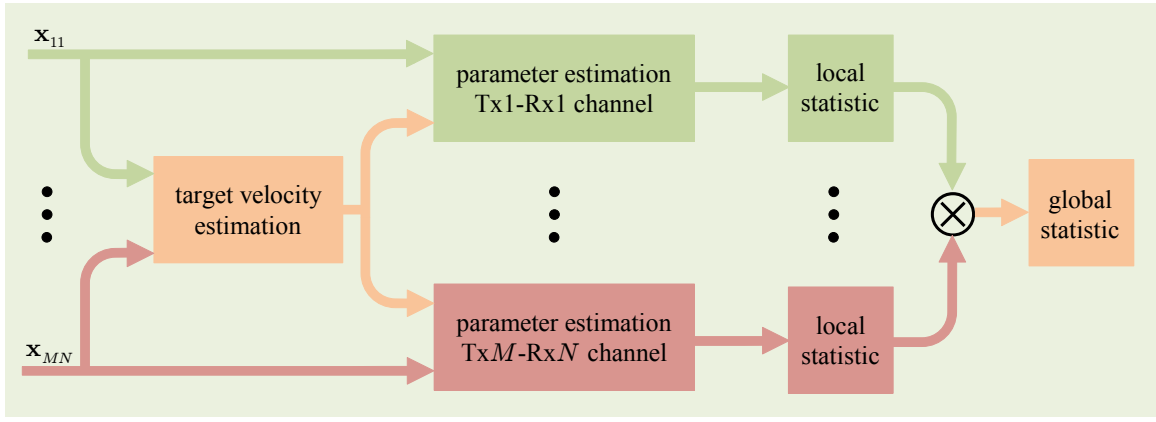


Figure 6. Parametric detector for distributed MIMO radar.

Table I
PARAMETERS USED IN SIMULATIONS OF DISTRIBUTED MIMO RADAR

M	N	f_c	K	T_r	$\sigma_{\alpha_{mn}}^2$	P_{mn}	v
2	2	1 GHz	32	2 ms	1	3	108 km/h

estimate (FPE) of the covariance matrix based on the following equation:

$$\hat{C}_{mn} = \frac{K}{L} \sum_{\ell=1}^L \frac{\mathbf{x}_{mn,\ell} \mathbf{x}_{mn,\ell}^H}{\mathbf{x}_{mn,\ell}^H \hat{M}_{mn}^{-1} \mathbf{x}_{mn,\ell}}, \quad (8)$$

which can be solved by iterative approaches [26].

The parametric MIMO-PGLRT, the covariance matrix based SCM, and the robust MIMO detector are compared with each other. The receiver operating characteristic (ROC) curves for the three detectors are shown in Fig. 7, where the parametric MIMO-PGLRT uses no training ($L = 0$), while two training sizes ($L = 36$ and $L = 64$) are considered for the SCM and robust MIMO detectors. The results are obtained when the disturbance signals are generated with different settings of clutter power and scatterer root-mean-square (RMS) velocity for different Tx-Rx pairs. This general clutter model [25], [48], which has been widely used to model the clutter Doppler characteristics and is not an AR process, is employed to evaluate the performance of the MIMO-PGLRT with model mismatch. The Parameters used in the simulation are listed in Table I. The clutter-to-noise ratio is 30 dB, and the signal-to-interference-plus-noise ratio (SINR) is 20 dB. The target velocity is 108 km/h with the moving direction randomly and uniformly chosen in the range $[-180^\circ, 180^\circ]$ for each simulation trial. The fluctuating target amplitudes α_{mn} are generated as complex Gaussian random variables with zero mean and variance $\sigma_{\alpha_{mn}}^2$. There are two transmitters at 0° and 65° relative to the target and two receivers at -30° and 40° . The clutter power and RMS values of the scatterer velocities are, respectively, selected as $[1.5, 0.8, 2, 1]$ and $[0.5, 1.5, 1.2, 0.8]$ m/s for the four Tx-Rx pairs. Note that the AR coefficients a_{mn} estimated for different Tx-Rx pairs are still different as the disturbance is non-homogeneous across Tx-Rx pairs.

Fig. 7 indicates that the covariance matrix based detectors benefit significantly from a larger training size. In particular,

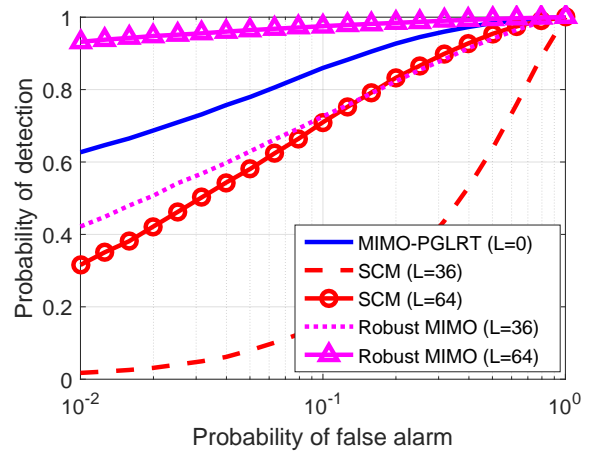


Figure 7. ROC curves for the MIMO-PGLRT detector, the SCM detector, and the robust MIMO detector in clutter with 2×2 antennas, $K = 32$ pulses, and $L = 0, 36, 64$ training data.

when $L = 2K = 64$, the robust MIMO detector outperforms the MIMO-PGLRT with $L = 0$, while the gap between the SCM and the MIMO-PGLRT is considerably smaller. The simulation results also demonstrate the advantage of the MIMO-PGLRT detector, which does not use any training signal, over the covariance matrix based detectors when the latter are supplied with limited training signals ($L = 36$). Specifically, the robust MIMO detector shows moderate performance loss compared to the MIMO-PGLRT detector, while the SCM detector fails to produce a detection. The advantage of the MIMO-PGLRT detector stems from the set of scalar AR models that take into account the non-homogeneous clutter variations from cell to cell. It is noted that covariance matrix based detectors often require $L \geq 2K$ homogeneous training signals to reach good detection performance [12].

IV. PARAMETRIC DETECTION FOR PASSIVE RADAR

Passive radar exploits non-cooperative illuminators of opportunity (IOs) to detect and track targets of interest without requiring a dedicated transmitter. Although passive radar has the advantages of covertness and deployment flexibility, passive sensing is more challenging than its active counterpart

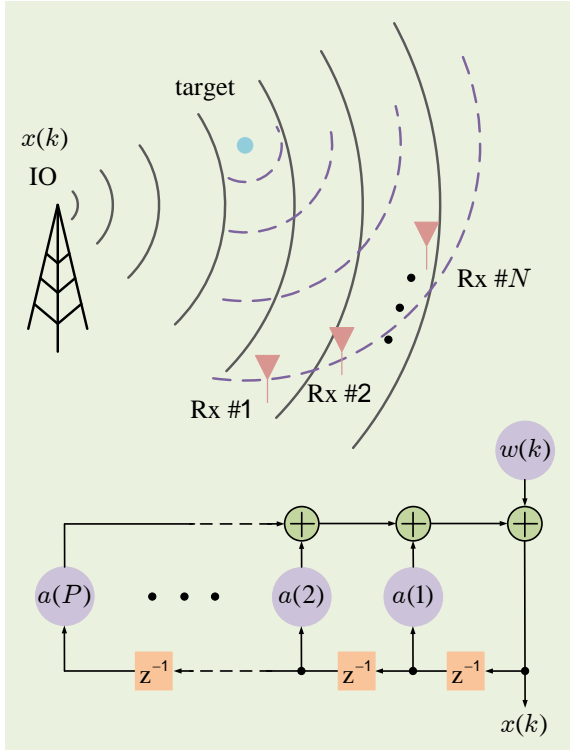


Figure 8. Configuration of a passive multistatic radar system.

because the transmitted signal is generally unknown at the receivers. Several research efforts have been spurred to address the target detection problem in passive multistatic radar [32], [33], [37].

Consider a multistatic passive radar system that consists of N geographically dispersed stationary receivers and one non-cooperative stationary transmitter located in a plane which also contains a moving target [37]. The waveform $x(t)$ transmitted by the IO impinges on the target and terminates at the receivers, forming a target signal with a bistatic delay of t_n and a Doppler frequency of f_n at the n -th receiver. In addition to the target echo, there is also a direct-path interference from the IO to the n -th receiver, with a propagation delay of d_n . We assume that any direct-path propagation is treated as interference. As a result, the system does not employ a reference antenna pointing to the IO direction to collect a reference IO signal. Fig. 8 provides an illustration of the setup. The dashed lines represent the reflection from the target and the solid lines are the transmission from the IO source. Since the location of the IO is usually known at each receiver, the direct-path induced delay d_n can be compensated to the target-path delay t_n , which gives $\tau_n \triangleq t_n - d_n$, where τ_n represents the propagation delay difference between the target-path and the direct-path at the n -th receiver. For simplicity, we assume the system is a stationary passive radar system (radar receivers are placed on stationary platforms), where the clutter has been filtered out in a pre-filtering stage.

Given the above discussions, the delay-compensated signal observed at the n -th receiver is given by

$$y_n(t) = \beta_n x(t) + \alpha_n x(t - \tau_n) e^{j2\pi f_n t} + \tilde{n}_n(t), \quad (9)$$

where β_n is the scaling coefficient which includes the antenna attenuation and the channel propagation effects from the IO to the n -th receiver, $\tilde{n}_n(t)$ contains the clutter and noise at the n -th channel, and α_n is the scaling coefficient accounting for the target reflectivity. Specifically, α_n lumps the target radar cross-section (RCS), the antenna gain, and channel propagation effects from the IO to the target and then from the target to the n -th receiver.

The IO waveform $x(t)$ has a duration of T_t seconds, e.g., due to framed transmissions employed by the IO, in which case T_t represents the frame duration. At the receiver end, the observation window T_o is chosen such that $T_o \geq T_t + \tau_{\max}$, where τ_{\max} denotes the maximum tolerated delay difference. Let the transmitted waveform have a bandwidth of B . Then, the received signal at each channel is sampled at frequency $f_s \geq 2(B + f_{\max})$, where f_{\max} is the maximum Doppler frequency of the target that is designed to be detectable by the passive system. The K samples of the observed signal are sequentially organized into an $K \times 1$ vector with $K = \lfloor T_o/T_s \rfloor$, where $T_s = 1/f_s$ denotes the sampling interval. Let $\mathbf{y}_n \in \mathbb{C}^{K \times 1}$ denote the sampled complex baseband signal at the n -th receiver, the target detection problem is to select between the following two hypotheses:

$$\begin{aligned} H_0 : \quad \mathbf{y}_n &= \beta_n \mathbf{x} + \mathbf{n}_n, \\ H_1 : \quad \mathbf{y}_n &= \beta_n \mathbf{x} + \alpha_n \mathcal{D}(\tau_n, f_n) \mathbf{x} + \mathbf{n}_n, \quad n = 1, \dots, N, \end{aligned} \quad (10)$$

where $\mathbf{x} \in \mathbb{C}^{K \times 1}$ contains the discrete samples of $x(t)$; $\mathcal{D}(\tau_n, f_n)$ is the delay-Doppler operator that accounts for the delay and Doppler shifts imparted to the IO signal as it propagates to the n -th receiver along the target path; $\mathbf{n}_n \in \mathbb{C}^{K \times 1}$ is the noise vector. Note that when multiplied by $\mathcal{D}(\tau_n, f_n)$, the signal \mathbf{x} is first converted into the frequency domain and then phase-shifted (in the frequency domain) due to the time domain delay τ_n . Then, it converts the delay-shifted signal back to the time domain and imposes a phase shift (in the time domain) caused by the Doppler frequency f_n .

The non-cooperative nature of passive sensing, i.e., the IO waveform \mathbf{x} is generally unknown, imposes an additional challenge in solving the passive detection problem in (10), when compared to its active counterpart. The IO waveform can be treated as a deterministic unknown vector to develop solutions, e.g., the energy detector (ED) and the generalized canonical correlation (GCC) detector [32]. However, the number of unknowns to be estimated in such detectors grows with the number of observations. Another method to avoid such a disadvantage is to model the IO waveform as an element-correlated stochastic process with unknown temporal correlation. Specifically, an AR model is used to fit the stochastic IO waveform where the temporal correlation is parameterized by the AR coefficients and the driving noise variance. A P -th order AR process is expressed as

$$x(k) = - \sum_{p=1}^P a(p)x(k-p) + w(k), \quad k = 1, \dots, \bar{K}, \quad (11)$$

where \bar{K} is the number of transmitted IO signal samples, $a(p)$ is the p -th AR coefficient with $\mathbf{a} = [a(1), \dots, a(P)]^T$, and

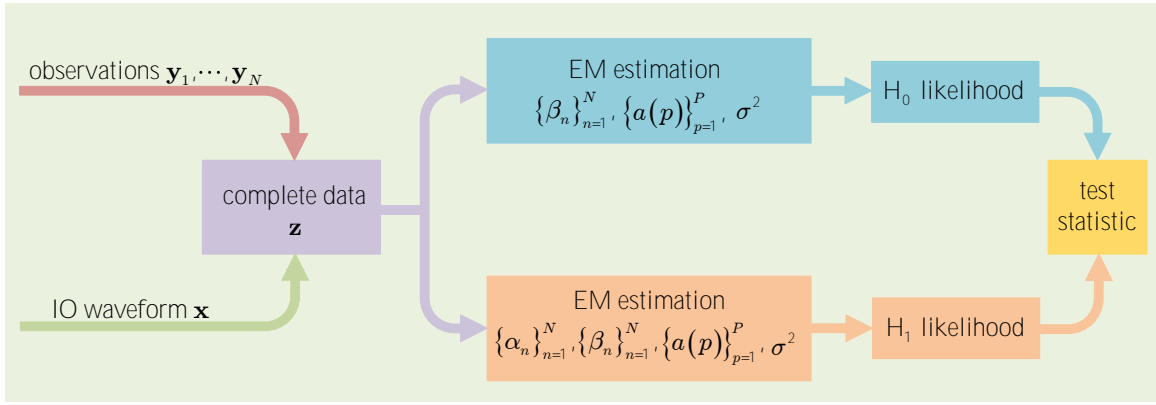


Figure 9. Parametric detector for passive multistatic radar.

$w(k) \sim \mathcal{CN}(0, \sigma^2)$ is the zero-mean driving noise. Note that $\bar{K} \leq K$, since the observation window T_o is selected to be no less than the time duration T_t of the transmitted signal with delay. Given (11), \mathbf{x} is zero-mean Gaussian distributed with covariance matrix $\mathbf{C}_x(\mathbf{a}, \sigma^2)$, which is Hermitian, Toeplitz, and thus can be fully determined by its first column, i.e., the auto-correlation function (ACF) sequence. In addition, the relationship between the AR parameters $\{a(p)\}_{p=1}^P$ and σ^2 , and the ACF sequence is described by the Yule-Walker equations [51]. Note that the AR model is introduced to model the IO waveform, which brings the advantage of capturing the waveform correlation and exploiting it to improve detection performance.

The AR model in (11) can be used to develop solutions for the passive detection problem in (10), i.e., a parametric detector. The ML estimations in the development of the detector turn out to be highly non-linear and do not have closed-form solutions [38]. An expectation-maximization (EM) procedure can be formulated to solve the estimation problem, and the estimates are subsequently used to derive a parametric GLRT detector. The EM algorithm alternatively iterates an expectation step and a maximization step until a convergence is achieved. Specifically, it first needs to determine the “complete” data as $\mathbf{z} = [\mathbf{x}^T, \mathbf{y}_1^T, \dots, \mathbf{y}_N^T]^T$ which includes both the unknown IO waveform and the observations from N receivers. After specifying the “complete” data, the EM algorithm starts with an initial guess of the unknown parameters $\{\alpha_n\}_{n=1}^N$, $\{\beta_n\}_{n=1}^N$, and AR parameters $\{a(p)\}_{p=1}^P$ and σ^2 under H_1 ; the unknown parameters under H_0 are the same as those of H_1 except for the target scaling coefficients $\{\alpha_n\}_{n=1}^N$. In fact, we only need to initialize the correlation matrix $\mathbf{C}_x(\mathbf{a}, \sigma^2)$ of the IO waveform instead of the AR parameters directly. A simple way is to initialize the covariance matrix to an identity matrix, which implies that the waveform correlation is ignored for the start of the EM algorithm. During each iteration of the EM algorithm, an expectation step (E-step) is followed by a maximization step (M-step) [37], [38]. In particular, the E-step is intended to find the expectation of the log-likelihood function (LLF) of the “complete” data \mathbf{z} , which is taken with respect to the signal waveform \mathbf{x} and conditioned on observations $\{\mathbf{y}_n\}_{n=1}^N$ given the estimates of the unknown parameters from the last iteration. Then, the

M-step is intended to maximize the expectation of the LLF with respect to the unknown parameters. The maximization is carried out sequentially with respect to each parameter group, including the scaling coefficients, the AR parameters, and the channel noise variance. When maximizing with respect to a specific group, the other parameters are fixed as the results from the last iteration or from the latest updates in this iteration. The iteration cycle is repeated until the algorithm converges, e.g., the difference of the estimates of the unknown parameters from the recent two iterations are smaller than a certain pre-defined tolerance level. Once the EM iteration converges, the final estimates of the unknown parameters can be substituted back into the likelihood ratio to compute the test statistic. The flowchart of the parametric detector for passive multistatic radar is shown in Fig. 9.

Since the detector is developed based on the assumption that the IO signal follows a scalar AR model, a mismatch may exist between the assumption and the exact IO signal. Fig. 10 reproduced here is for the case of a frequency modulation (FM) signal that is employed as the IO waveform to test the performance of the detectors. It illustrates the gains provided by the parametric GLRT (curve labeled “pGLRT”), which exploits the waveform correlation by modeling the IO signal as an AR process, over conventional detectors. For comparison purposes, three conventional detectors are also included in the analysis. The “clairvoyant MF” curve comes from the matched filtering (MF) detector assuming that the IO waveform is perfectly known, which serves as an upper bound for all passive detectors considered in this section. The “mGCC” stands for the modified version of the original GCC detector, which was developed in the absence of direct path interference (DPI) [32]. The modification is carried out by adding a DPI cancellation step which subtracts the estimated DPI from the original observation to obtain the modified observation and replacing the original observation in the existing detector with the modified one (see [37, Section 4.1] for details). Finally, the “sGLRT” represents the simple GLRT where the covariance matrix \mathbf{C}_x is replaced by an identity matrix, i.e., the correlation of the IO waveform is completely ignored. It is observed that the performance of the pGLRT detector is close to the upper bound provided by the clairvoyant MF and the sGLRT detector performs 2 dB worse than the pGLRT detector in our setup.

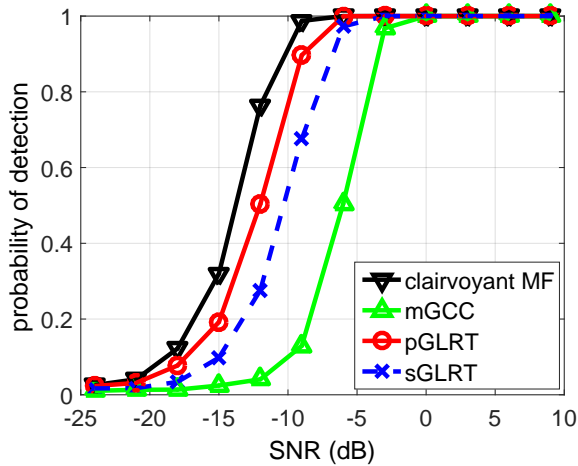


Figure 10. Detection performance of the parametric GLRT versus the target SNR using an FM waveform as the IO with $N = 3$ receivers. In the simulation, the AR model order is estimated as $P = 1$ based on the generalized Akaike information criterion (AIC) [50]. The target delays are $[2.2, 3.6, 4.9]T_s$ for the three paths, the target Doppler are $[3.1, 0.8, -3.6] \frac{f_s}{K}$, the SNR of the direct signal is 0 dB, and the probability of false alarm is set to 10^{-2} .

V. CONCLUSIONS

In this survey article, we have shown that AR processes can be employed to model the clutter and unknown source signal to reduce the requirement of training data for effective target detection. There are some subtle differences in applying parametric modeling in solving different radar detection problems. Specifically, in phased-array radar, the disturbance is modeled as multi-channel AR process. For distributed MIMO radar, a set of independent scalar AR processes are used to model the clutter observed at different Tx-Rx pairs, which are capable of capturing the variations in both clutter structure and power level across different probing-observing angles. Finally, for passive radar, the unknown IO signal is treated as an element-correlated stochastic process, which can be represented by an AR model. In all cases, we have demonstrated that AR modeling is able to bring significant performance improvement over conventional non-parametric methods, in particular when training data is limited.

REFERENCES

- [1] L. C. Potter, R. Carriere, and M. J. Gerry, "A GTD-based parametric model for radar scattering," *IEEE Transactions on Antennas and Propagation*, vol. 43, no. 10, pp. 1058–1067, Oct 1995.
- [2] P. Bharadwaj, P. Runkle, L. Carin, J. A. Berrie, and J. A. Hughes, "Multiaspect classification of airborne targets via physics-based HMMs and matching pursuits," *IEEE Transactions on Aerospace and Electronic Systems*, vol. 37, no. 2, pp. 595–606, April 2001.
- [3] K. J. Sangston and A. Farina, "Coherent radar detection in compound-Gaussian clutter: Clairvoyant detectors," *IEEE Aerospace and Electronic Systems Magazine*, vol. 31, no. 11, pp. 42–63, November 2016.
- [4] M. Greco, F. Bordon, and F. Gini, "X-band sea-clutter nonstationarity: influence of long waves," *IEEE Journal of Oceanic Engineering*, vol. 29, no. 2, pp. 269–283, April 2004.
- [5] M. Rangaswamy and J. H. Michels, "A parametric multichannel detection algorithm for correlated non-Gaussian random processes," in *Proceedings of the 1997 IEEE National Radar Conference*, Syracuse, NY, May 1997, pp. 349–354.
- [6] A. L. Swindlehurst and P. Stoica, "Maximum likelihood methods in radar array signal processing," *Proceedings of the IEEE*, vol. 86, no. 2, pp. 421–441, Feb 1998.
- [7] J. R. Roman, M. Rangaswamy, D. W. Davis, Q. Zhang, B. Himed, and J. H. Michels, "Parametric adaptive matched filter for airborne radar applications," *IEEE Transactions on Aerospace and Electronic Systems*, vol. 36, no. 2, pp. 677–692, April 2000.
- [8] P. Wang, H. Li, and B. Himed, "A new parametric GLRT for multichannel adaptive signal detection," *IEEE Transactions on Signal Processing*, vol. 58, no. 1, pp. 317–325, Jan 2010.
- [9] G. Alfano, A. D. Maio, and A. Farina, "Model-based adaptive detection of range-spread targets," *IEE Proceedings - Radar, Sonar and Navigation*, vol. 151, no. 1, pp. 2–10, Feb 2004.
- [10] P. Wang, Z. Wang, H. Li, and B. Himed, "Knowledge-aided parametric adaptive matched filter with automatic combining for covariance estimation," *IEEE Transactions on Signal Processing*, vol. 62, no. 18, pp. 4713–4722, 2014.
- [11] I. S. Reed, J. D. Mallett, and L. E. Brennan, "Rapid convergence rate in adaptive arrays," *IEEE Transactions on Aerospace and Electronic Systems*, vol. AES-10, no. 6, pp. 853–863, Nov 1974.
- [12] E. J. Kelly, "An adaptive detection algorithm," *IEEE Transactions on Aerospace and Electronic Systems*, vol. AES-22, no. 2, pp. 115–127, March 1986.
- [13] K.J. Sohn, H. Li, and B. Himed, "Parametric GLRT for multichannel adaptive signal detection," *IEEE Transactions on Signal Processing*, vol. 55, pp. 5351–5360, Nov 2007.
- [14] J. Guerci, *Space-Time Adaptive Processing for Radar, Second Edition*, ser. Artech House radar library. Artech House Publishers, 2014.
- [15] W. Melvin, M. Wicks, P. Antonik, Y. Salama, P. Li, and H. Schuman, "Knowledge-based space-time adaptive processing for airborne early warning radar," *IEEE Aerospace and Electronic Systems Magazine*, vol. 13, no. 4, pp. 37–42, April 1998.
- [16] D. J. Rabideau and A. O. Steinhardt, "Improved adaptive clutter cancellation through data-adaptive training," *IEEE Transactions on Aerospace and Electronic Systems*, vol. 35, no. 3, pp. 879–891, July 1999.
- [17] P. Wang, H. Li, and B. Himed, "Bayesian radar detection in interference," in *Modern Radar Detection Theory*, A. De Maio and M. S. Greco, Eds. The Institution of Engineering and Technology, 2015, pp. 133–164.
- [18] J. Li, G. Liu, N. Jiang, and P. Stoica, "Moving target feature extraction for airborne high-range resolution phased-array radar," *IEEE Transactions on Signal Processing*, vol. 49, no. 2, pp. 277–289, Feb 2001.
- [19] Y. Gao, H. Li, and B. Himed, "Adaptive Subspace Tests for Multichannel Signal Detection in Auto-Regressive Disturbance," *IEEE Transactions on Signal Processing*, vol. 66, no. 21, pp. 5577–5588, Nov 2018.
- [20] F. Colone and F. Filippini, "Autoregressive Model Based Polarimetric Adaptive Detection Scheme Part I: Theoretical Derivation and Performance Analysis," *IEEE Transactions on Aerospace and Electronic Systems*, vol. 56, no. 5, pp. 3762–3778, Oct. 2020.
- [21] F. Colone and F. Filippini, "Autoregressive Model Based Polarimetric Adaptive Detection Scheme Part II: Performance Assessment Under Spectral Model Mismatch," *IEEE Transactions on Aerospace and Electronic Systems*, vol. 56, no. 5, pp. 3779–3795, Oct. 2020.
- [22] C. Jiang, H. Li and M. Rangaswamy, "Conjugate gradient parametric adaptive matched filter," in *2010 IEEE Radar Conference*, Arlington, VA, May 2010, pp. 740–745.
- [23] C. Jiang, H. Li and M. Rangaswamy, "Conjugate gradient parametric detection of multichannel signals," *IEEE Transactions on Aerospace and Electronic Systems*, vol. 48, no. 2, pp. 1521–1536, Apr. 2012.
- [24] A. M. Haimovich, R. S. Blum, and L. J. Cimini, "MIMO radar with widely separated antennas," *IEEE Signal Processing Magazine*, vol. 25, no. 1, pp. 116–129, 2008.
- [25] Q. He, N. H. Lehmann, R. S. Blum, and A. M. Haimovich, "MIMO radar moving target detection in homogeneous clutter," *IEEE Transactions on Aerospace and Electronic Systems*, vol. 46, no. 3, pp. 1290–1301, July 2010.
- [26] C. Y. Chong, F. Pascal, J. Ovarlez, and M. Lesturgie, "MIMO radar detection in non-Gaussian and heterogeneous clutter," *IEEE Journal of Selected Topics in Signal Processing*, vol. 4, no. 1, pp. 115–126, Feb 2010.
- [27] P. Chen, L. Zheng, X. Wang, H. Li, and L. Wu, "Moving target detection using colocated MIMO radar on multiple distributed moving platforms," *IEEE Transactions on Signal Processing*, vol. 65, no. 17, pp. 4670–4683, 2017.
- [28] P. Wang, H. Li, and B. Himed, "Moving target detection using distributed MIMO radar in clutter with nonhomogeneous power," *IEEE Transactions on Signal Processing*, vol. 59, no. 10, pp. 4809–4820, 2011.
- [29] P. Wang, H. Li, and B. Himed, "A parametric moving target detector for distributed MIMO radar in non-homogeneous environment," *IEEE*

Transactions on Signal Processing, vol. 61, no. 9, pp. 2282–2294, May 2013.

- [30] H. Li, Z. Wang, J. Liu, and B. Himed, “Moving target detection in distributed MIMO radar on moving platforms,” *IEEE Journal of Selected Topics in Signal Processing*, vol. 9, no. 8, pp. 1524–1535, 2015.
- [31] H. D. Griffiths and C. J. Baker, “Passive coherent location radar systems. part 1: performance prediction,” *IEE Proceedings - Radar, Sonar and Navigation*, vol. 152, no. 3, pp. 153–159, June 2005.
- [32] K. S. Bialkowski, I. V. L. Clarkson, and S. D. Howard, “Generalized canonical correlation for passive multistatic radar detection,” in *2011 IEEE Statistical Signal Processing Workshop (SSP)*, Nice, France, June 2011, pp. 417–420.
- [33] D. E. Hack, L. K. Patton, B. Himed, and M. A. Saville, “Detection in passive MIMO radar networks,” *IEEE Transactions on Signal Processing*, vol. 62, no. 11, pp. 2999–3012, June 2014.
- [34] J. Liu, H. Li, and B. Himed, “On the performance of the cross-correlation detector for passive radar applications,” *Signal Processing*, vol. 113, pp. 32 – 37, 2015.
- [35] G. Cui, J. Liu, H. Li, and B. Himed, “Signal detection with noisy reference for passive sensing,” *Signal Processing*, vol. 108, pp. 389 – 399, 2015.
- [36] M. Rashid and M. Naraghi-Pour, “Multitarget Joint Delay and Doppler-Shift Estimation in Bistatic Passive Radar,” *IEEE Transactions on Aerospace and Electronic Systems*, vol. 56, no. 3, pp. 1795–1806, June 2020.
- [37] X. Zhang, H. Li, and B. Himed, “Multistatic passive detection with parametric modeling of the IO waveform,” *Signal Processing*, vol. 141, pp. 187 – 198, 2017.
- [38] F. Wang, H. Li, X. Zhang, and B. Himed, “Signal parameter estimation for passive bistatic radar with waveform correlation exploitation,” *IEEE Transactions on Aerospace and Electronic Systems*, vol. 54, no. 3, pp. 1135–1150, 2018.
- [39] J. Wang, L. Wang, J. Sheng, C. Fu, H. Wang, and C. Zhou, “Passive Distributed Aperture Radar Imaging Method Based on Unknown Waveform Modeling,” in *2019 6th Asia-Pacific Conference on Synthetic Aperture Radar (APSAR)*, Xiamen, China, Nov 2019, pp. 417–420.
- [40] M. A. Richards, *Fundamentals of radar signal processing*, 2nd ed. New York, NY, USA: McGraw-Hill, 2014.
- [41] J. R. Guerci and E. J. Baranoski, “Knowledge-aided adaptive radar at DARPA: an overview,” *IEEE Signal Processing Magazine*, vol. 23, no. 1, pp. 41–50, 2006.
- [42] B. Himed, “MCARM/STAP data analysis,” Air Force Research Laboratory Final Technical Report, AFRL-SN-RS-TR-1999-48, Vol. II (of two), May 1999.
- [43] O. Saleh, M. Ravan, R. Riddolls, and R. Adve, “Fast fully adaptive processing: a multistage STAP approach,” *IEEE Transactions on Aerospace and Electronic Systems*, vol. 52, no. 5, pp. 2168–2183, 2016.
- [44] H. Wang and L. Cai, “On adaptive spatial-temporal processing for airborne surveillance radar systems,” *IEEE Transactions on Aerospace and Electronic Systems*, vol. 30, no. 3, pp. 660–670, July 1994.
- [45] J. H. Michels, B. Himed, and M. Rangaswamy, “Robust STAP detection in a dense signal airborne radar environment,” *Signal Processing*, vol. 84, no. 9, pp. 1625 – 1636, 2004, special Section on New Trends and Findings in Antenna Array Processing for Radar.
- [46] F. C. Robey, D. R. Fuhrmann, E. J. Kelly, and R. Nitzberg, “A CFAR adaptive matched filter detector,” *IEEE Transactions on Aerospace and Electronic Systems*, vol. 28, no. 1, pp. 208–216, Jan 1992.
- [47] E. Fishler, A. Haimovich, R. S. Blum, L. J. Cimini, D. Chizhik, and R. A. Valenzuela, “Spatial Diversity in Radars-Models and Detection Performance,” *IEEE Transactions on Signal Processing*, vol. 54, no. 3, pp. 823–838, March 2006.
- [48] M. I. Skolnik, *Introduction to Radar Systems*, 3rd ed. New York, NY: McGraw-Hill, 2001.
- [49] N. J. Willis, *Bistatic Radar*, 2nd ed. Raleigh, NC: SciTech Publishing, 2005.
- [50] T. Söderström and P. Stoica, *System Identification*. London, UK: Prentice Hall International, 1989.
- [51] S. M. Kay, *Modern Spectral Estimation: Theory and Application*. Englewood Cliffs, NJ: Prentice Hall, 1988.



Fangzhou Wang (S'13) received the B.S. and M.S. degrees from Beijing Institute of Technology, Beijing, China in 2012 and 2015, respectively, both in electrical engineering. He is currently pursuing the Ph.D. degree in electrical engineering at Stevens Institute of Technology, Hoboken, NJ, USA. He has been a Teaching and Research Assistant in the Department of Electrical and Computer Engineering, Stevens Institute of Technology, Hoboken, NJ, USA, since 2015. His research interests include statistical signal processing and convex optimization, with emphasis on wireless communications and radar signal processing.

Mr. Wang received the Outstanding Research Assistant Award in 2018 from Stevens Institute of Technology. He is a frequent reviewer for *IEEE Transactions on Signal Processing*, *IEEE Transactions on Aerospace and Electronic Systems*, *IEEE Transactions on Wireless Communications*, *IEEE Signal Processing Letters*, and *IEEE Wireless Communications Letter*.



Pu Wang (S'05-M'12-SM'18) received the Ph.D. degree in Electrical Engineering from the Stevens Institute of Technology, Hoboken, NJ, USA, in 2011.

He is now a Principal Research Scientist at the Mitsubishi Electric Research Laboratories (MERL), Cambridge, MA, where he was an intern in the summer of 2010. Before returning to MERL, he was a Research Scientist at the Schlumberger-Doll Research, Cambridge, MA, contributing to developments of next-generation logging-while-drilling Acoustics/NMR products. His current research inter-

ests include signal processing, Bayesian inference, machine learning, and their applications to (mmWave and THz) sensing, wireless communications, networks and automotive applications.

Dr. Wang was selected as a Distinguished Speaker of the Society of Petrophysicists and Well Log Analysts (SPWLA) in 2017. He was a recipient of the IEEE Jack Neubauer Memorial Award from the IEEE Vehicular Technology Society in 2013. He also received the Outstanding Doctoral Thesis in Electrical Engineering Award in 2011, the Edward Peskin Award in 2011, the Francis T. Boesch Award in 2008, and the Outstanding Research Assistant Award in 2007 from the Stevens Institute of Technology. He is an Associate Editor for *IEEE Signal Processing Letters*.



Xin Zhang (S'17-M'17) received his B.Eng. degree (with honors) from University of Science and Technology Beijing (USTB), China, in 2008, and M.Eng. degree from Beijing University of Posts and Telecommunications (BUPT), China, in 2011, both in electrical engineering. In May 2017, he became a Ph.D. in electrical engineering at Stevens Institute of Technology (SIT), Hoboken, NJ, USA.

From 2011 to 2017, he worked as a research and teaching assistant in the Signal Processing and Communication (SPAC) Laboratory, Department of Electrical and Computer Engineering, SIT. His research interests include statistical signal processing, optimization algorithm applications, passive sensing, and wireless communications. From 2017 to 2019, he was a senior RF application engineer with LitePoint, a Teradyne company, in Sunnyvale, CA. From 2019 to present, he works on automotive radar signal processing as a radar system engineer in Aptiv.



Hongbin Li (M'99-SM'08-F'19) received the B.S. and M.S. degrees from the University of Electronic Science and Technology of China, in 1991 and 1994, respectively, and the Ph.D. degree from the University of Florida, Gainesville, FL, in 1999, all in electrical engineering.

From July 1996 to May 1999, he was a Research Assistant in the Department of Electrical and Computer Engineering at the University of Florida. Since July 1999, he has been with the Department of Electrical and Computer Engineering, Stevens Institute of Technology, Hoboken, NJ, where he is currently the Charles and Rosanna Batchelor Memorial Chair Professor. He was a Summer Visiting Faculty Member at the Air Force Research Laboratory in the summers of 2003, 2004 and 2009. His general research interests include statistical signal processing, wireless communications, and radars.

Dr. Li received the IEEE Jack Neubauer Memorial Award in 2013 from the IEEE Vehicular Technology Society, Outstanding Paper Award from the IEEE AFICON Conference in 2011, Provost's Award for Research Excellence in 2019, Harvey N. Davis Teaching Award in 2003, and Jess H. Davis Memorial Research Award in 2001 from Stevens Institute of Technology, and Sigma Xi Graduate Research Award from the University of Florida in 1999. He has been a member of the IEEE SPS Signal Processing Theory and Methods Technical Committee (TC) and the IEEE SPS Sensor Array and Multichannel TC, an Associate Editor for *Signal Processing* (Elsevier), *IEEE Transactions on Signal Processing*, *IEEE Signal Processing Letters*, and *IEEE Transactions on Wireless Communications*, as well as a Guest Editor for *IEEE Journal of Selected Topics in Signal Processing* and *EURASIP Journal on Applied Signal Processing*. He has been involved in various conference organization activities, including serving as a General Co-Chair for the 7th IEEE Sensor Array and Multichannel Signal Processing (SAM) Workshop, Hoboken, NJ, June 17-20, 2012. Dr. Li is a member of Tau Beta Pi and Phi Kappa Phi.



Dr. Braham Himed (F'07) received his Engineer Degree in electrical engineering from Ecole Nationale Polytechnique of Algiers in 1984, and his M.S. and Ph.D. degrees both in electrical engineering, from Syracuse University, Syracuse, NY, in 1987 and 1990, respectively. Dr. Himed is a Division Research Fellow with the Air Force Research Laboratory, Sensors Directorate, Distributed RF Sensing Branch, in Dayton Ohio, where he is involved with several aspects of radar developments. His research interests include detection, estimation, multichannel

adaptive signal processing, time series analyses, array processing, adaptive processing, waveform diversity, MIMO radar, passive radar, and over the horizon radar. Dr. Himed is the recipient of the 2001 IEEE region I award for his work on bistatic radar systems, algorithm development, and phenomenology. He is a Fellow of the IEEE and a past Chair of the AESS Radar Systems Panel. He is the recipient of the 2012 IEEE Warren White award for excellence in radar engineering. Dr. Himed is also a Fellow of AFRL (Class of 2013).